Civil Engineering

Analysis of a database of instrumented static load tests on continuous flight auger piles in tropical soils

http://dx.doi.org/10.1590/0370-44672023780128

Aleones José da Cruz Junior[1,5]
https://orcid.org/0000-0003-0422-1911
Juan Félix Rodríguez Rebolledo[1,6]
https://orcid.org/0000-0003-2929-7381
Heitor Cardoso Bernardes[2,7]
https://orcid.org/0000-0003-2053-5240
Daniel Magalhães da Cruz[3,8]
https://orcid.org/0000-0001-8734-0371
Maurício Martines Sales[4,9]
https://orcid.org/0000-0003-1331-3121

[1]Universidade de Brasília – UnB,
Departamento de Engenharia Civil e Meio Ambiente,
Brasília - Distrito Federal - Brasil.

[2]Instituto Federal Goiano,
Rio Verde - Goiás - Brasil.

[3]Universidade Federal do Rio Grande do Sul – UFRGS,
Departamento de Engenharia Mecânica,
Porto Alegre - Rio Grande do Sul - Brasil.

[4]Universidade Federal de Goiás – UFG,
Escola de Engenharia Civil e Meio Ambiente,
Goiânia - Goiás - Brasil.

E-mails : [5]aleones.junior@ifgoiano.edu.br,
[6]jrodriguezr72@hotmail.com,
[7]heitor.bernardes@ifgoiano.edu.br,
[8]daniel.cruz@ufrgs.br, [9]sales.mauricio@gmail.com

Abstract

This article assesses the behavior of full-scale static load tests (SLTs) conducted with instrumentation for strain measurements, in order to provide insights into the pile load transfer curves along its length. A collection of instrumented SLTs from a specific region offers a valuable dataset for the geotechnical community, which can be leveraged for machine learning-based neural network studies and probabilistic-statistical analysis, ultimately enhancing the reliability of regional semi-empirical methods. This study presents an analysis of a database containing the results of 80 instrumented SLTs conducted on CFA (continuous flight auger) piles in the metropolitan area of Goiânia, Goiás, Brazil, spanning from 2016 to 2022. It establishes correlations between the pile's maximum skin friction (q_l^{max}) and soil resistance, as well as between the pile shaft and pile base resistances, and relative displacement at the pile-soil interface (δ_{int}). The geotechnical surveys accompanying each SLT are also included in the database under examination, aiding in the definition of a representative geotechnical profile of Goiânia's soil. The q_l^{max} values derived from the database exhibit significant dispersion compared to the semi-empirical methods commonly employed in Brazil. Additionally, these values span a broad range of δ_{int}, with considerably lower values for the superficial, porous, and structured layer of sandy clay compared to the deeper layers.

Keywords: piles, static load test, instrumentation, skin friction, geotechnical database.

1. Introduction

Currently, the execution of a static load test (SLT) is the most reliable method for collecting data to verify the foundation agreement with the ultimate and serviceability requirements of the designed pile foundation. This type of test cannot be easily replaced because it verifies the pile behavior in true scale, considering very similar geotechnical characteristics and the same installation procedure that the real foundation will be subjected to during its lifetime. Also, for the review of the ultimate limit states, the Brazilian Foundation Standard NBR 6122 (ABNT, 2019) establishes a 20% reduction of the coefficients for the calculation of bearing capacity of piles when results of SLT are available, obtaining a more efficient and economical foundation.

In the Brazilian Central-Western region, foundation designers have increasingly been requesting the implementation of instrumented SLTs for strain measurements. This approach aims to maximize the quantity of information gathered concerning pile behavior. Instrumentation enables the examination of the pile load transfer curve, skin friction mobilization, and the maximum load capacity at the pile tip. This, in turn, facilitates a more cost-effective and secure approach to geotechnical and structural pile design.

For instance, consider the Brazilian Foundation Standard NBR 6122 (ABNT, 2019) for CFA piles, which establishes an upper limit for pile base resistance force in relation to the calculated skin friction (for ultimate limit state analysis). With the results from instrumented SLTs, it becomes possible to assess these load components with greater accuracy.

Data obtained from an instrumented SLT can also serve to fine-tune the parameters within the geotechnical model for deeper soil layers. This is particularly valuable, since obtaining samples for laboratory tests from these deeper layers is a more complex and costly procedure. By leveraging finite element analysis for a reverse analysis of the SLT data and the load transfer curves obtained through pile instrumentation, it becomes possible to enhance the assessment of variations in the strength and stiffness of the soil layers along the depth of the pile (Bernardes *et al.*, 2022).

Given the aforementioned benefits, the Brazilian standard NBR 6122 (ABNT, 2019) defines that SLTs must be conducted in foundations with more than 100 CFA piles, with a quantity equal to at least 1% of the total number of elements. This guideline has been adhered to in the design of foundations in Brazil, facilitating the accumulation of a substantial volume of test results that can subsequently be utilized to construct comprehensive SLT databases.

Alonso (2000, 2002, 2004) gathered the results of 202 SLTs in CFA piles in Brazil. Marcos *et al.* (2012) organized the results of 400 SLTs performed in 16 countries, which can be used for statistical analysis or reference values to assist in the interpretation of tests in nearby locations. Galbraith *et al.* (2014) tabulate the results of 175 static SLTs carried out in Ireland, to verify the statistical variability of the pile load capacity.

The main SLT database currently available, is the Deep Foundation Load Test Database (DFLTD), in the USA, is maintained by the Federal Highway Administration (Petek *et al.*, 2016). This database contains more than 1500 SLTs, which have been collected and stored for different pile types and soil conditions. The DFLTD was compiled and treated in different studies to provide a repository of reliable deep foundation data (Abu-Hejleh *et al.*, 2015; Kalavar & Ealy, 2000; Satyanarayana *et al.*, 2001).

As Information Technology continues to evolve, many geotechnical problems previously deemed intricate can now be addressed through the integration of artificial intelligence. This progress underscores the need for utilizing Machine Learning algorithms and accessing well-structured extensive datasets (big data). Consequently, compiling reliable databases has gained significance, as they are essential for the development of methodologies based on machine learning. Such methodologies include Bayesian approaches (Zhang *et al.*, 2020) and neural networks (Pham *et al.*, 2020) applied to pile design.

This article presents an analysis of a database encompassing findings from 80 instrumented SLTs performed on CFA piles within the metropolitan area of Goiânia, Goiás, Brazil, spanning the years 2016 to 2022. It reveals various correlations between pile and soil resistance, as well as between pile resistance and normalized settlement. These correlations can be advantageous for geotechnical engineers. By making this dataset accessible in a publicly available repository, the aim is to foster the widespread use of this information within the technical community, be it for research purposes or for the preliminary design of geotechnical structures in this region.

2. Materials and methods

The SLTs were conducted in tropical soils in the central-west region of Brazil, in the state of Goiás, within the metropolitan area of Goiânia, at 39 different sites, spread over an area with a radius of around 5 km. The coordinates of each site, followed by the main characteristics of the tests, including pile diameter (D), pile length (L), maximum applied load to the pile (P_{max}), water level depth (WT, measured from the top of the pile), and the thickness of the excavated soil layer preceding the test execution, are accessible through the dataset provided by Cruz Junior & Sales (2023).

All the SLTs were static, performed with slow maintained loading, using a series of equal load increments, according to the Brazilian standards NBR 12131 (ABNT, 2006) and its subsequent revision NBR 16903 (ABNT, 2020). None of the SLTs included unloading-reloading events, due to their potential influence on the assessment of pile stiffness and the interpretation of strain-gauge records, which are affected by the occurrence of residual strains (Fellenius & Nguyen, 2019).

All the piles were instrumented for strain measurements, utilizing force transducers in the form of miniaturized load cells, developed according to the design by Cruz Junior (2016). Geometric compatibility was assumed between the deformations registered by the sensors and the CFA pile in which they were installed. 90º rosette-type electrical strain gauges with a resistance of 120 ohms, self-temperature-compensated to mitigate temperature influences, were affixed to the instrumented bars. These bars were mounted in a full-bridge circuit configuration to measure axial deformations. To minimize inaccuracies caused by cable resistance, a six-wire bridge configuration was employed. The instrumented bars, constructed from an aluminum alloy, measured 135 mm in height and 12.85 mm in diameter. A two-component epoxy-based adhesive, recommended for precise and prolonged tests, was used to fix the strain gauges securely.

All instruments underwent calibration using three controlled loading and unloading cycles in the laboratory, subjecting them to stresses up to 70 MPa, with deformations recorded by the data acquisition system. The data acquisition equipment facilitated signal reading and adjustment for initial balance (zero balance), definition of sensitivity factor, excitation voltage, gain, and range.

The tested piles were solely of the Continuous Flight Auger (CFA) type, varying in lengths from 12 to 29 meters and diameters from 0.5 to 0.9 meters. Each pile had the sensors affixed to the steel cage near its top (see Figure 1a) and to bundled steel bars extending deeper towards the tip (see Figure 1b), promptly installed after the concrete placement.

The Secant Stiffness Method (Lam & Jefferis, 2011) was employed to calculate stress values at various depths of each pile based on strain measurements. This method considers the variation of the concrete stiffness modulus with the stress level throughout the pile's cross-section. It has undergone extensive testing and is strongly recommended for analyzing instrumented SLTs (Fellenius, 2012; Lam & Jefferis, 2011). In all the tested piles, a minimum of two reference load cells were installed at the pile's top, as depicted in Figure 1a, and at locations approximately one or two diameters below the pile cap.

The analyzed database (Cruz Junior & Sales, 2023) includes load data at various depths (measured from the pile top) as well as pile settlements for all 80 SLTs. A majority of these tests were carried out with ten loading stages, although the number of stages could be adjusted based on the pile's geotechnical and structural response during the test.

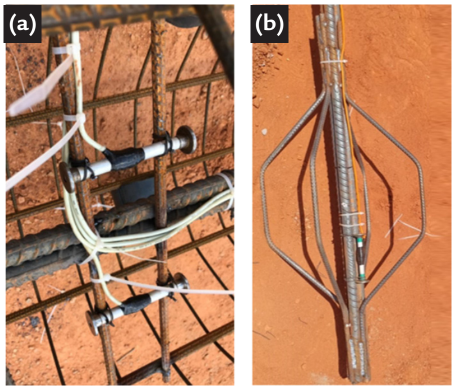

Figure 1 - Typical installation of load cells in the steel cage: (a) reference sensors at the pile top, and (b) at the pile tip.

All sites employed the Standard Penetration Test (SPT) as the method for geotechnical profile characterization, conducted by reputable companies with expertise in the geotechnical field and in accordance with the requirements of the Brazilian standard NBR 6484 (ABNT, 2001). The examined database shows that for each SLT, an SPT sounding considered representative was selected based on proximity or project reliability. From these soundings, data on soil type (determined by visual-tactile classification) and NSPT values per meter were obtained. These data reveal a consistent geotechnical soil profile observed in 96% of the tests, as illustrated in Figure 2, with the exception of SLTs 14, 15, and 16, which exhibit distinct profiles.

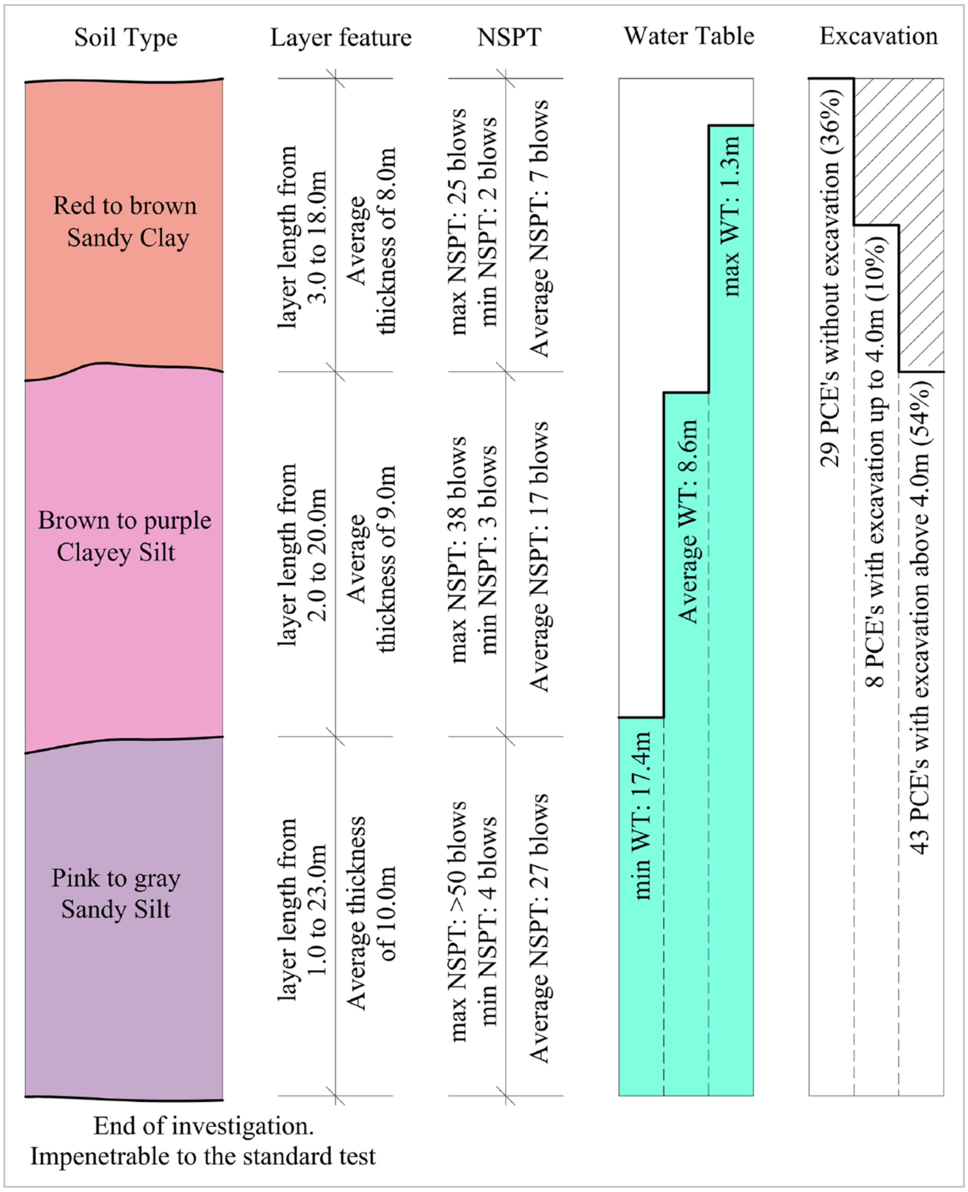

Figure 2 - Typical geotechnical profile verified in the SLTs.

Figure 2 shows a superficial layer of red sandy clay that presents N_{SPT} values ranging from 2 to 25. This soil consists of a porous and structured matrix, a common characteristic in the Brazilian Central-West region (Rebolledo *et al*., 2019). Then, an intermediate layer predominately composed of a residual clayey silt, with an average N_{SPT} value of 17. Lastly, there is a layer of pink to gray micaceous sandy silt with an average N_{SPT} value of 27, underlain by an impermeable rock mass consisting of micaschists and granulites. The thickness of these three layers varies according to the typical profile shown in Figure 2. Romão (2006) described a similar general geotechnical profile for the city of Goiânia.

The N_{SPT} values shown in Figure 2 exhibit a wide range, with coefficients of variation of 70%, 50%, and 48% for the sandy clay, silty clay, and sandy silt layers, respectively. These values do not significantly exceed the coefficients of variation for N_{SPT} results reported in literature, which vary between 15% and 54% (Kulhawy, 1992; Uzielli, 2008; Kwak *et al*., 2010; Bernardes, 2021). The variability of N_{SPT} observed in this study reflects the results of boreholes conducted at various locations within a 5 km radius. While tactile and visual classifications have shown some consistency in layer types.

The significant variance among the obtained N_{SPT} values comes mainly from the following factors:

1) Soil discontinuity, heterogeneity and anisotropy.

2) Superficially, there may be a layer of fill material or a crust formed by the soil's wetting and drying cycles at the survey site. These layers were not distinguished during classification.

3) Tropical soils result from rock weathering, leading to the presence of altered rock fragments in certain areas, which can indeed impact N_{SPT} values.

4) Climate can also affect surface layers: during the rainy season, soil resistance decreases significantly due to water's influence on soil structure. This disrupts cementing connections between particles and reduces matric suction. Conversely, in the dry season, the structure remains stable, and matric suction notably increases.

The authors suggest that factors 2 and 4 could be the primary drivers behind the observed data dispersion in the surface layer.

The unitary pile skin friction (q_l) value was determined by calculating the difference in measured loads between two instrumented levels and then dividing it by the lateral area of the pile, assuming a constant cross-sectional area. The values of q_l initially increase with each applied load increment at the top until they reach a maximum value (q_l^{max}), which is generally asymptotic and may be followed by a reduction to a residual value. This maximum value represents the limit of resistance. Thus, an instrumented layer associated with a soil type was defined between each pair of sensors based on the visual-tactile classifications from the boreholes. In total, 253 layers with q_l values were obtained for each load increment, and q_l^{max} values were determined for 126 of these layers. In most cases, the q_l^{max} values were obtained progressively from the top to the tip of the pile.

The unitary pile base pressure (q_b) was determined from the loads measured at the last sensor, placed as close as possible to the pile tip, and was divided by the cross-sectional area of the pile. In some tests, it was not possible to install the strain gauges at the tip of the pile due to difficulties during the insertion of the pile steel cage. In these cases, the strain gauges were positioned between 2 and 4 meters above the tip, and the pile base pressure was linearly extrapolated based on the measured skin friction. The qb values also increased with the applied load increments at the top and rarely exhibited a tendency toward an asymptotic limit value.

3. Analysis and results

3.1 Correlations between pile and soil strength

To investigate the relation between pile and soil strength for each SLT, the value of q_l^{max} was plotted against the average N_{SPT} values for the same layer. Figure 3 shows these results for different soil types defined in Figure 2, including layers composed of sandy clay (Figure 3a), clayey silt (Figure 3b), and sandy silt (Figure 3c). The q_l^{max} values were measured for each soil layer, where the convergence of the unitary skin friction to a maximum value was observed. Additionally, Figure 4 has been included to aid in the comparative analysis between the semi-empirical predictions and the measured q_l^{max} values.

Figure 3 also shows the linear regression of the measured values (Fit, red dotted line), along with the three lines representing q_l^{max} as a function of the N_{SPT} values, calculated using traditional semi-empirical approaches widely used in national practice for the specific plie type, soil composition, and SPT values, namely Décourt & Quaresma (1978) (D-Q), Antunes & Cabral (1996) (A C), and Aoki & Velloso (1975) (A-V). The equations and the empirical coefficients used in each of these methods are described in the Appendix.

The results for the sandy clay showed the larger dispersion ($R^2 = 0.55$, Figure 3a). The variability in the results primarily stems from the factors discussed in Section 2. Furthermore, in certain instances, the q_l value, particularly in the surface layer, could be impacted by previous basement excavations conducted before the load test. The semi-empirical methods of A-C and A-V underestimated the values of q_l^{max}obtained through linear regression of the measured points (dotted red line), which is evident in Figures 4b and 4c, respectively. The D-C method exhibited slightly better agreement with the measured data (Figure 4a). The research conducted by Zheng *et al*. (2012) indicates that piles situated in excavations in sand with a non-dilatant pile-soil interface experience a reduction in shaft capacity of 16 to 20% compared to those constructed at the surface. Conversely, for piles with a dilatant pile-soil interface, the shaft capacity shows an increase ranging from 22 to 44%. Therefore, in order to enhance comprehension and refine the aforementioned methodologies, conducting research to investigate the behavior of piles in such soil conditions within excavations of varying depths is imperative. Zheng's findings suggest that the surface soil-pile interface (sandy clay) exhibits a more dilatant behavior, as indicated by discrepancies between predicted values and SLT.

Figure 3b shows that the q_l^{max} measurements for the clayey silt presented a better correlation with the N_{SPT} values ($R^2 = 0.71$) over a wider range (between 3 to 38 blows) than that shown in Figure 3a. This confirms that superficial layers are influenced by a greater number of factors compared to the deeper layers. The linear fit provides reasonably accurate estimates of the q_l^{max} values, with predictions similar to those of the A-C method (Figure 4f). The D-Q and A-V methods exhibited a tendency to overestimate (Figure 4d) and underestimate (Figure 4e) the measured data, respectively.

The linear regression that shows the best agreement with the measured q_l^{max} values is the one obtained for the sandy silt (R^2 = 0.85, Figure 3c). It is once again confirmed that as the layer depth increases, there is a significant decrease in the dispersion of values. However, Figures 4g, 4h and 4i show that the three semi-empirical methods overestimate the pile q_l^{max} in the SM soil, at least considering the analyzed N_{SPT} range (between 4 and 50).

The behavior described above shows that in the geotechnical profile of Goiânia, the semi-empirical design methods tend to underestimate the shaft resistance of the pile's upper portion and overestimate the resistance of the pile in the deeper layers, usually composed of sandy silt soil. Since such semi-empirical methods are extensively used in the foundation design in the region, it is possible that the underestimated strength of the pile's upper portion is compensated by the overestimation of the lower portions, which may lead to a pile resistance close to those verified in the field, showing a quite wrong load distribution along the pile length.

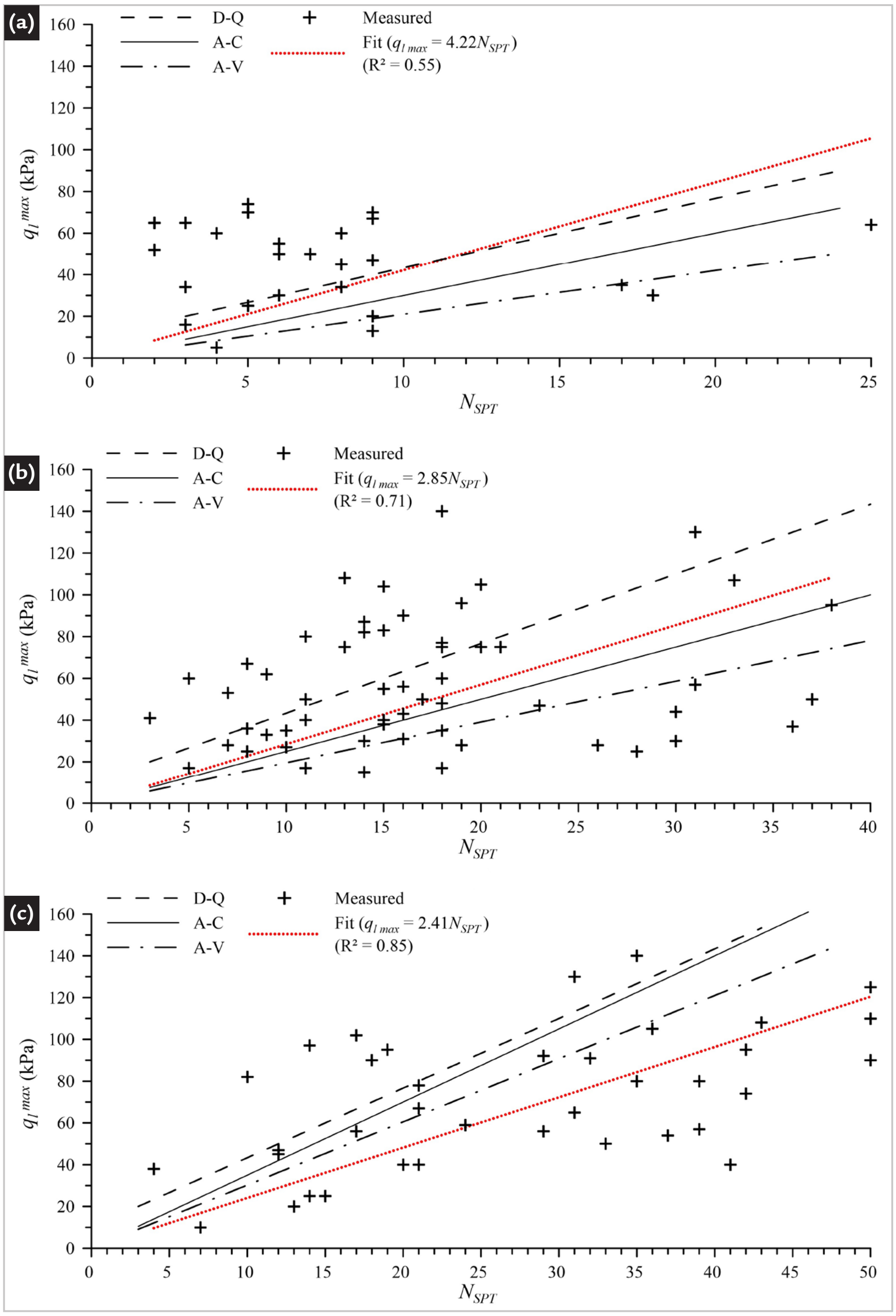

Figure 3 - Correlations between the N_{SPT} and the q_l^{max} values for different soil types: (a) sandy clay, (b) clayey silt, and (c) sandy silt.

This reinforces the need for using load tests to validate semi-empirical results in foundation design and highlights the necessity to refine the three mentioned methods for improved accuracy when applied in a regional context.

It was not possible to plot the graph for the maximum stresses measured at the pile base (q_b^{max}), since the soil beneath the pile base is classified as impenetrable to the SPT test in most of the tests (N_{SPT} > 50). Furthermore, it's important to note that some of the SLTs did not achieve full mobilization of the pile base load capacity, primarily due to limitations in the reaction system.

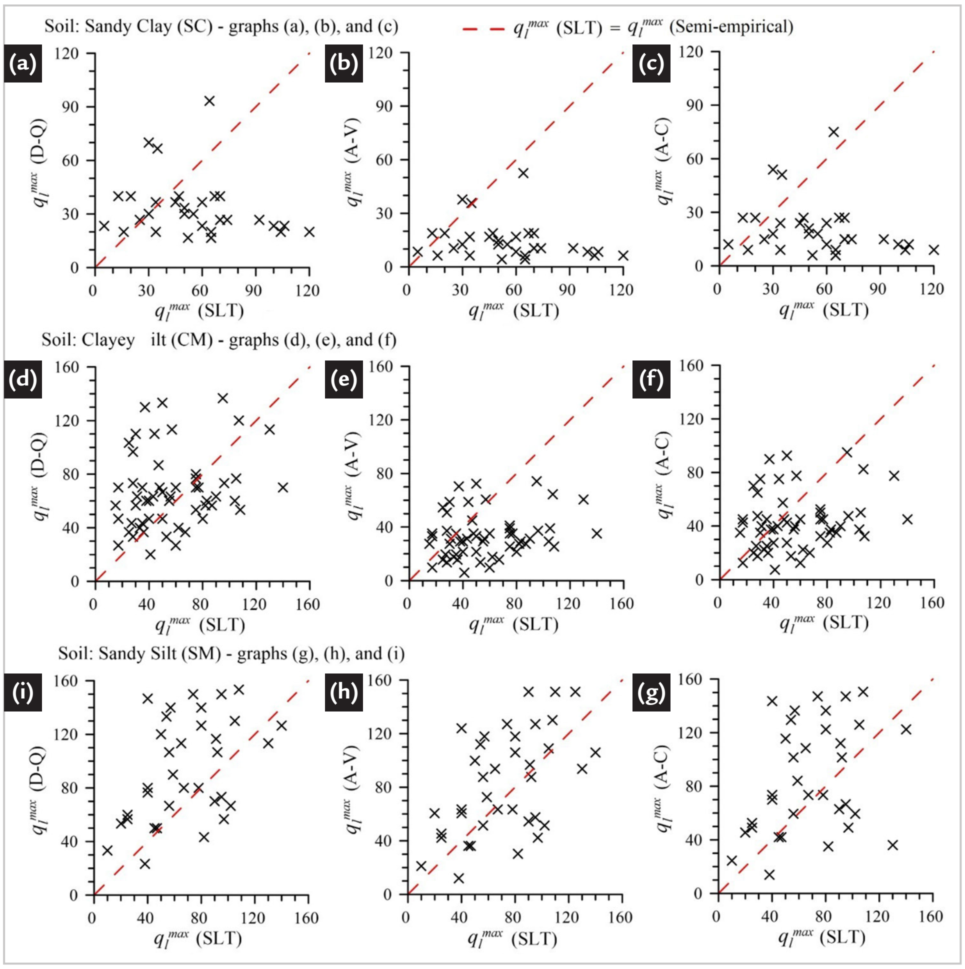

Figure 4 - Relationship between the q_l^{max} obtained by the SLTs and the q_l computed by the different semi-empirical methods and types of soil considered values for different soil types.

However, when considering an average N_{SPT} value greater than 50 and only the SLTs that reached maximum mobilization of the pile base (a total of 17 SLTs), an average value of q_l^{max} = 3.68 MPa and a standard deviation equal to 1.97 MPa was calculated. Despite the fact that all these tests were conducted in sandy silt soil, the significant standard deviation of the sample suggests that relying on semi-empirical methods based on the SPT test is not advisable for estimating q_b^{max} in soils with N_{SPT} values exceeding 50.

3.2 Displacement required for the maximum skin friction mobilization

The relative displacement at the pile-soil interface (δ_{int} / D) required for maximum mobilization of the skin friction is one of the uncertainty factors for pile design, needed, for example, for the application of load-transfer curves methods (Liu *et al*., 2004; Ni *et al*., 2017). The increase of δ_{int} during the pile loading depends on many factors, including: the installation method, soil type, density and consolidation state, among others (Bohn *et al*., 2017).

Thus, the SLTs database was used to investigate the relative displacement required for full mobilization of skin friction in CFA piles constructed in tropical soils. For each SLT that achieved q_l^{max} at a given depth, the value of δ_{int} / D was computed by subtracting the pile's elastic shortening from the settlements measured at the top. The elastic shortening was computed using the axial load-transfer curves obtained from the strain-gauges.

Histograms were plotted, showing the number of SLTs that exhibited the mobilization of q_l^{max} within defined δ_{int} / D intervals for a given soil layer (Figure 5). To determine which probability distribution (Normal, Lognormal, Beta, or Gamma) best fit the sample, the Kolmogorov-Smirnov test was employed (Berger & Zhou 2014). The test identified the Lognormal distribution as the best fit, with a critical distance statistic ranging between 0.07 and 0.08 for different soil types. The sample mean ($\overline{\delta_{int}}$) and standard deviation (S.D.), and the Lognormal distributions for the samples collected in each soil type are shown in Figure 5.

Integrating the area beneath the Lognormal distribution to reach a probability of around 80%, the correspondent δ_{int} / D values are smaller than 10, 16 and 40 mm, for the sandy clay (Figure 5a), clayey silt (Figure 5b), and sandy silt (Figure 5c), respectively. Tomlinson & Woodward (2008) report δ_{int} / D values, between 0.3 and 1% (to reach q_l^{max}). These reference values correspond to δ_{int} ranging from 1.5 and 9 mm given the different pile diameters used in the SLTs (between 0.5 and 0.9 m), which are in accordance with the ones shown in Figure 5a. However, Figures 5b and 5c show larger δ_{int} values.

The data analysis showed that the pile diameter does not have influence on the δ_{int} value, at least for the given diameter range, between 0.5 and 0.9 m. For this reason, the δ_{int} values presented in Figure 5 were not normalized by the pile diameter.

The larger δ_{int} values required for the mobilization of q_l^{max} in Figures 5b and 5c are probably related to the soil type –

among many other aspects, such as the soil density, consolidation state and the great variation in resistance in the layers – in which the q_l^{max} can occur in different loading stages, and following different mobilization patterns. Figure 6 exemplifies this behavior, showing the graphs of the unitary skin friction mobilization (q_l) versus δ_{int} for each soil layer of the SLT No. 72.

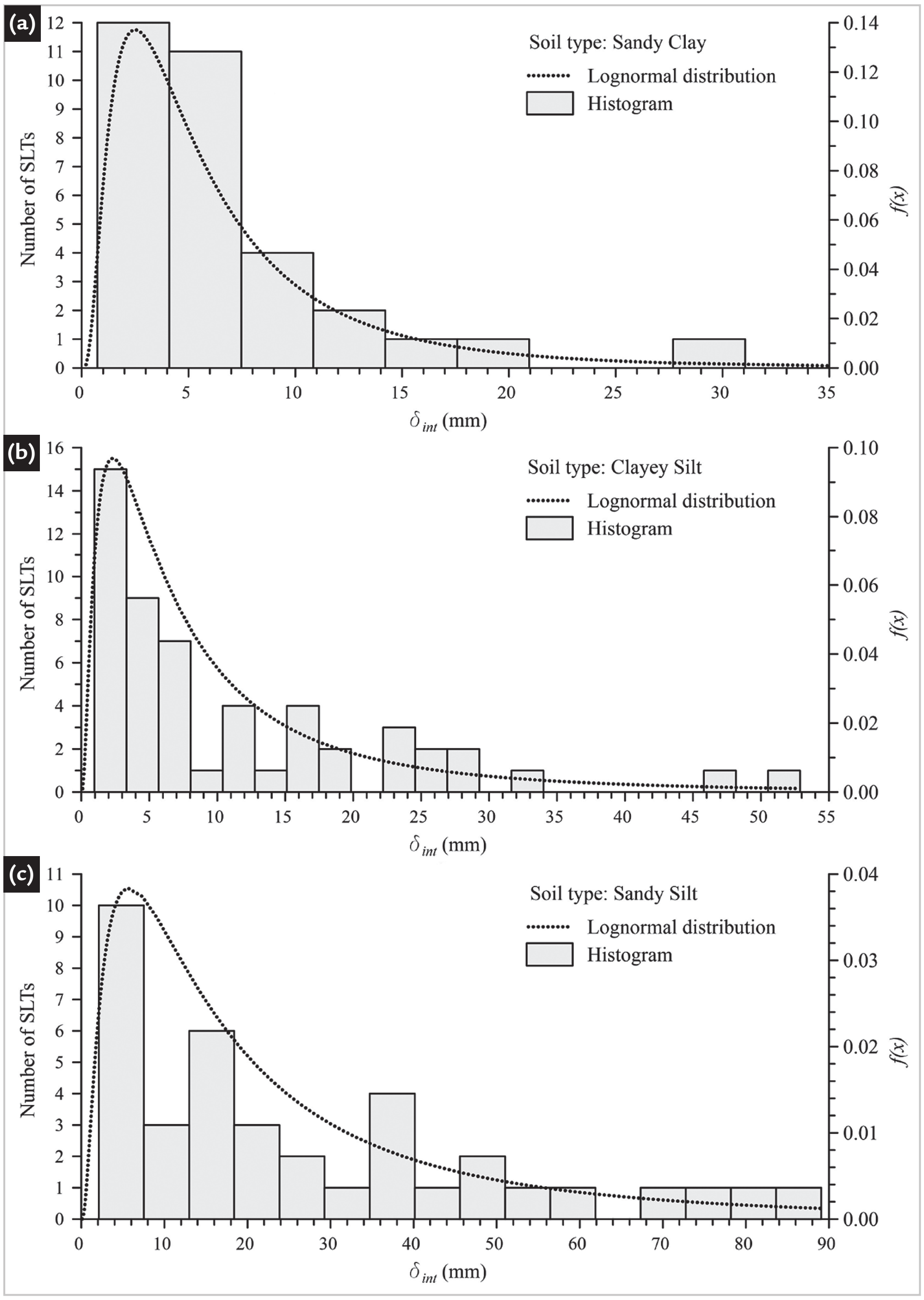

Figure 5 - Histograms of the number of SLTs that present q_l^{max} values in different ranges of δi_{nt}, for different soil layers: (a) sandy clay, (b) clayey silt, and (c) sandy silt.

Figure 6a shows a q_l vs. δ_{int} curve with a peak resistance at the 5th loading stage, followed by a subsequent drop in q_l. In this stage, the mobilized ql in the soil layer immediately below is still increasing (clayey silt, Figure 6b), reaching its maximum value only in the 8th loading stage. For the deeper soil layer, q_l^{max} occurs at the 7th stage (sandy silt, Figure 6c).

In a single pile vertically loaded at the top and installed in a hypothetical homogeneous soil profile, the maximum peak resistance of each soil layer will always be mobilized from the top to the bottom of the pile (Fellenius, 2018; Joshi *et al.*, 1989; Poulos & Davis, 1968). However, the constitutive differences between the layers of the geotechnical profile studied herein caused the mobilization of q_l^{max} of the sandy silt layer (between -13 and -21m, Figure 6b) prior to the immediately above layer (clayey silt, between -7.5 and -13 m, Figure 6c).

In this case, note that despite the skin friction of the pile being fully mobilized by the end of the test, the compressive stress at the base (q_b) continues to increase and shows no signs of converging towards a maximum asymptotic value. This behavior of load transfer mechanisms for lateral friction and tip resistance is predicted in the papers by Cambefort (1964) and Mussara & Massad (2015). According to Cambefort's first law, the pile has already reached a limit of lateral resistance, while Cambefort's second law suggests that with increased loading at the pile top, the soil at the tip level reacts along the pseudo-elastic portion, potentially leading the load-settlement curve to revert to a linear pattern.

The occurrence of peak resistance in the q_l vs. δ_{int} graphs of the SLT database was recorded in 47% of the sandy clay samples (top layer) considered in Section 3.2. In the underlying layers, the clayey silt and sandy silt soils exhibited q_l vs. δ_{int} curves showing peak resistance in 36% and 33% of their respective samples. Subsequently, the increase in ql before and after reaching the peak value can be associated with soil hardening behavior, while the decrease q_l observed post-peak may indicate a softening response, as reported by Ong *et al.* (2021). Additionally, the rise in qb with displacement (hardening) without reaching a peak value could be linked to punching shear failure of the pile tip, as discussed by Vesic (1972) concerning deep foundations (*L/D* > *5*).

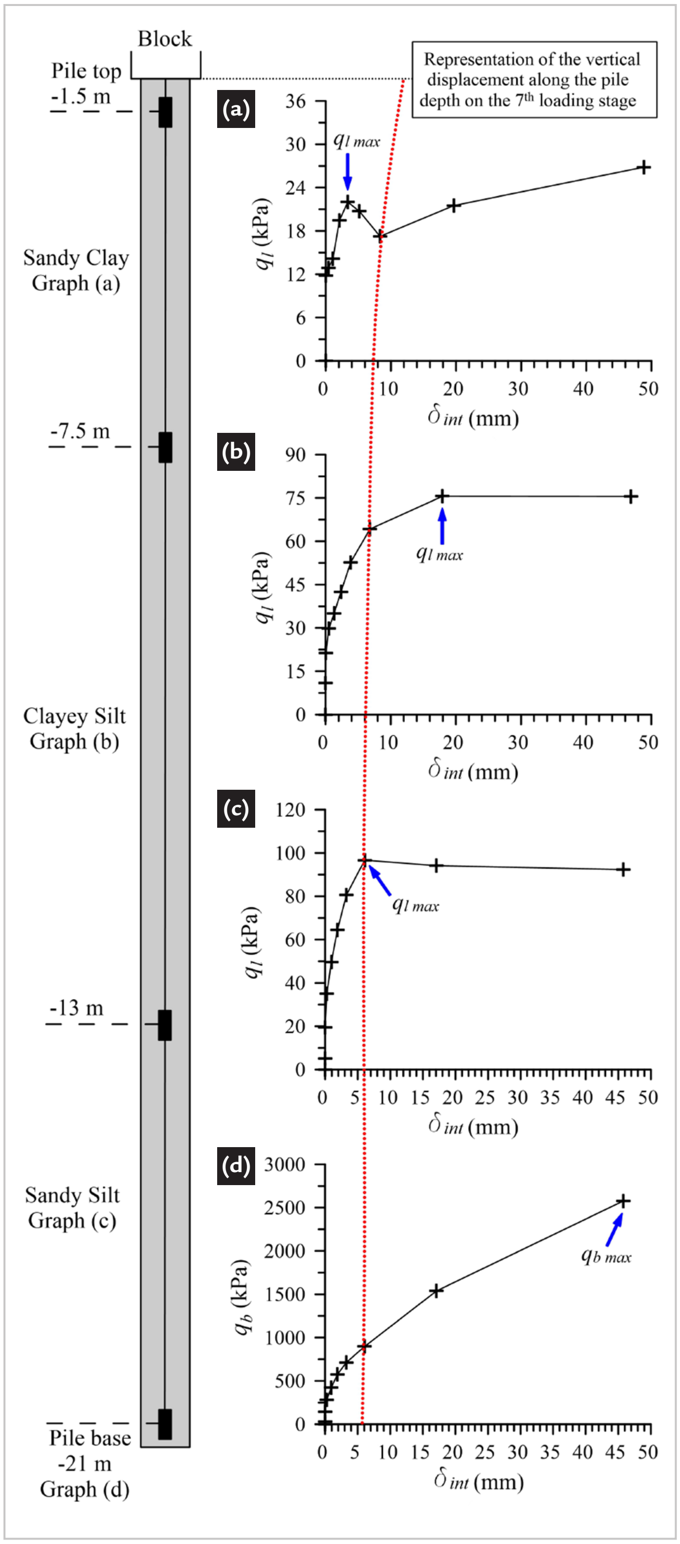

Figure 6 - Graphs of q_l vs. δ_{int} for different soil types: (a) sandy clay, (b) clayey silt, and (c) sandy silt; and (d) q_l vs. δ_{int} for the pile base (SLT-72).

4. Conclusion

This article presents an analysis of the results of 80 instrumented SLTs conducted on Continuous Flight Auger (CFA) piles in Goiânia, Brazil. The data used in the analysis are part of the publicly available database provided by Cruz Junior & Sales (2023). The database also contains information on the soil profile and the N_{SPT} values at each meter of depth, which has been utilized in the analyses. With these data now accessible to the geotechnical engineering community, various types of research, including machine learning-based neural network studies and statistical analyses, can be conducted to enhance the accuracy of regional semi-empirical methods for calculating load-bearing capacity and estimating the initial stiffness of piles.

Empirical correlations were proposed to estimate the pile maximum skin friction as a function of the N_{SPT} values for the three more common soil types present in the geotechnical profile of Goiânia, however, they should be used only as preliminary guidance due to the variability in N_{SPT} values. The D-Q and A-C semi-empirical methods reasonably estimated the q_l^{max} measured for the sandy clay and clayey silt soils, respectively. For the sandy silt (deeper layer) soil, all the semi-empirical methods overestimated the pile's skin resistance. The proposed correlations may be useful for estimating the q_l^{max} of CFA piles built in tropical soils, in preliminary design stage, and for the development of regional semi-empirical methods.

The study of skin friction mobilization as a function of the displacement at the pile-soil interface shows that q_l^{max} values occur under a wide range of δ_{int}, with the q_l^{max} mobilization possibly occurring in the soil deeper layer before the intermediate one. In a typical soil profile of Goiânia, the SLTs show that the δ_{int} values are much smaller for the superficial, porous, and structured sandy clay layer than for the deeper ones.

Acknowledgments

The authors thank the Universidade de Brasília, the Universidade Federal de Goiás, and the Instituto Federal de Educação, Ciência e Tecnologia Goiano (IFGoiano) for the support and infrastructure that enabled this research. The authors also acknowledge the Coordenação de Aperfeiçoamento de Pessoal de Nível Superior (CAPES) and the Conselho Nacional de Desenvolvimento Científico e Tecnológico (CNPq) for financial support and collaboration.

List of symbols and abbreviations

D: Pile diameter
L: Pile length
N_{SPT}: number of blows measured on a SPT test
P_{max}: Maximum load applies in a pile in the load test
q_b^{max}: Maximum compressive stresses acting at the pile base
q_l^{max}: Maximum value of the unitary pile skin friction
SLT: Static load test
ST: Soil type
WT: Water table (measured from the pile top)
δ_{int}: Relative displacement at the pile-soil interface

References

ABU-HEJLEH, N. M.; ABU-FARSAKH, M.; SULEIMAN, M. T.; TSAI, C. Development and use of high-quality databases of deep foundation load tests. ***Transportation Research Record: Journal of the Transportation Research Board***, v. 2511, n. 1, p. 27-36. 2015. DOI: https://doi.org/10.3141/2511-04.

ALONSO, U. R. Complementação do banco de dados de provas de carga estáticas em estacas hélice contínua. *In*: CONGRESSO BRASILEIRO DE MECÂNICA DOS SOLOS E ENGENHARIA GEOTÉCNICA, 12., 2002, São Paulo. ***Anais*[...]** 1557-1568.

ALONSO, U. R. Complementação do banco de dados de provas de carga estáticas em estacas hélice contínua. *In*: SEMINÁRIO DE ENGENHARIA DE FUNDAÇÕES ESPECIAIS E GEOTECNIA, 5., 2004, São Paulo. ***Anais*[...]** 1: 517-526.

ALONSO, U. R. Contribuição para a formação de um banco de dados de provas de carga estáticas em estacas hélice contínua. *In*: SEMINÁRIO DE ENGENHARIA DE FUNDAÇÕES ESPECIAIS E GEOTECNIA, 4., 2000, São Paulo. ***Anais*[...** 2: 430-450.

ANTUNES, W. R.; CABRAL, D. A. Capacidade de carga em estacas hélice contínua. In: SEMINÁRIO DE ENGENHARIA DE FUNDAÇÕES E GEOTECNIA, 3., 1996, São Paulo. Anais[...] 2: 105-109.

AOKI, N.; VELLOSO, D. A. An approximate method to estimate the bearing capacity of piles. *In*: PAN-AMERICAN CONFERENCE ON SOIL MECHANICS AND FOUNDATION ENGINEERING - PACSMFE, 5. 1975, Buenos Aires. ***Anais*[...** 1: 367-376.

ASSOCIAÇÃO BRASILEIRA DAS NORMAS TÉCNICAS - ABNT. ***NBR 6122***: Projeto e execução de fundações. Rio de Janeiro: ABNT, 2019.

ASSOCIAÇÃO BRASILEIRA DAS NORMAS TÉCNICAS - ABNT. ***NBR 6484***: Solo - sondagens de simples reconhecimento com SPT - método de ensaio. Rio de Janeiro: ABNT, 2020.

ASSOCIAÇÃO BRASILEIRA DAS NORMAS TÉCNICAS - ABNT. ***NBR 12131***: Estacas - prova de carga estática - método de ensaio. Rio de Janeiro: ABNT, 2006.

ASSOCIAÇÃO BRASILEIRA DAS NORMAS TÉCNICAS - ABNT. ***NBR 16903***: Solo - Prova de carga estática em

fundação profunda. Rio de Janeiro: ABNT, 2020.
BERNARDES, H. C. Aplicação de análise probabilística ao cálculo de capacidade de carga de estacas hélice contínua. ***Revista de Engenharia Civil IMED,*** v. 8, n. 1, p. 53-68, 2021. https://doi.org/10.18256/2358-6508.2021.v8i1.3459.
BERNARDES, H. C.; SALES, M. M.; MACHADO, R. R.; CRUZ JUNIOR, A. J. da; CUNHA, R. P. da; RESENDE, Angelim, R.; REBOLLEDO, J. F. R. Coupling hardening soil model and Ménard pressuremeter tests to predict pile behavior. ***European Journal of Environmental and Civil Engineering,*** v. 26, n. 11, p. 5221-5240. 2022. DOI: https://doi.org/10.1080/19648189.2021.1886180.
BOHN, C., SANTOS, A. Lopes dos; FRANK, R. Development of axial pile load transfer curves based on instrumented load tests. ***Journal of Geotechnical and Geoenvironmental Engineering,*** 143(1), 1–15. 2017. https://doi.org/10.1061/(ASCE)GT.1943-5606.0001579.
CAMBEFORT, M. Essai sur le comportement em terrain homogène des pieux isolés et des groupes de pieux. Annales - L'INSTITUTE DU BATIMENT ET DES TRAVAUX PUBLIC, n. 204, p. 1478-1518, Dec. 1964.
CINTRA, J. C. A.; AOKI, N. ***Fundações por estacas*:** projeto geotécnico. Oficina de Textos. São Paulo, 2010, 93 p.
CRUZ JÚNIOR, A. J. ***Instrumentação de fundações estaqueadas.*** Dissertação (Mestrado em Geotecnia, Estruturas e Construção) - Universidade Federal de Goiás. Goiânia, 2016. 208 f.
CRUZ JUNIOR, A. J.; SALES, M. M. ***Banco de dados de provas de carga estática instrumentada.*** Relatório técnico. Universidade Federal de Goiás. Goiânia, 2023, 40 p. Available at: https://files.cercomp.ufg.br/weby/up/142/o/Relat%C3%B3rio_-_Banco_de_Provas_de_Carga_Estatica_Instrumentadas_-_UFG-IFGoiano_-_REV01.pdf
DÉCOURT, L.; QUARESMA, A. R. Capacidade de carga de estacas a partir de valores de SPT. *In*: CONGRESSO BRASILEIRO DE MECÂNICA DOS SOLOS E ENGENHARIA DE FUNDAÇÕES-COBRAMSEF, 6., 1978, Rio de Janeiro. Anais[...] p. 45-53.
FELLENIUS, B. H. Discussion of critical assessment of pile modulus determination methods. ***Canadian Geotechnical Journal,*** v. 49, n.5, p. 614-621, 2012. DOI: https://doi.org/10.1139/t2012-027.
FELLENIUS, B. H. Discussion of development of axial pile load transfer curves based on instrumented load tests. ***Journal of Geotechnical and Geoenvironmental Engineering,*** v. 144, n. 4, p. 2-6. 2018. DOI: https://doi.org/10.1061/(ASCE)GT.1943-5606.0001867.
FELLENIUS, B. H. NGUYEN, B. N. Common mistakes in static loading-test procedures and result analyses. ***Geotechnical Engineering Journal of the SEAGS & AGSSEA.*** v. 50, Sept., 2019, p. 20-31.
GALBRAITH, A. P.; FARRELL, E. R.; BYRNE, J. J. Uncertainty in pile resistance from static load tests database. ***Proceedings of the Institution of Civil Engineers - Geotechnical Engineering,*** v. 167, n. 5, p. 431-446, 2014. DOI: https://doi.org/10.1680/geng.12.00132.
JOSHI, R. C.; SHARMA, H. D.; SPARROW, D. Skin friction distribution along driven piles. *In*: INTERNATIONAL CONFERENCE ON SOIL MECHANICS AND FOUNDATION ENGINEERING, 12., 1989, Rio de Janeiro. ***Anais*[...]** 929-932.
KALAVAR, S.; EALY, C. FHWA Deep Foundation Load Test Database. *In*: NEW TECHNOLOGICAL AND DESIGN DEVELOPMENTS IN DEEP FOUNDATIONS, 2000, Reston, VA. ***Anais*[...]** American Society of Civil Engineers, 192-206. 2000. DOI: https://doi.org/10.1061/40511(288)14.
KULHAWY, F. H. On the evaluation of soil properties. ***ASCE Geotech. Spec. Publ.*** n. 31, p. 95-115, 1992.
KWAK, K.; KIM, K. J.; HUH, J.; LEE, J. H.; PARK, J. H. Reliability-based calibration of resistance factors for static bearing capacity of driven steel pipe piles. ***Canadian Geotechnical Journal,*** v. 47, n. 5, p. 528-538, 2010. DOI: https://doi.org/10.1139/T09-119.
LAM, C.; JEFFERIS, S. A. Critical assessment of pile modulus determination methods. ***Canadian Geotechnical Journal,*** v. 48, n. 10, p. 1433-1448. 2011.DOI: https://doi.org/10.1139/T11-050
LIU, J.; XIAO, H. B.; TANG, J.; LI, Q. S. Analysis of load-transfer of single pile in layered soil. ***Computers and Geotechnics,*** v. 31, n. 2, p. 127-135, 2004. DOI: https://doi.org/10.1016/j.compgeo.2004.01.001.
MARCOS, M. C.; LIN, S. S.; LIAO, M. R.; HUANG, J. K.; CHEN, Y. J. Development of a database for pile load tests. *In*: GEOCONGRESS 2012, 2012, Reston, VA. ***Anais*[...]** American Society of Civil Engineers, 295–304. American Society of Civil Engineers. 2012. DOI: https://doi.org/10.1061/9780784412121.031.
MUSARRA, M.; MASSAD, F. Static load tests in an instrumented rock socket barrette pile. ***Soils and Rocks,*** v. 38, n. 2, p. 163-177, 2015. DOI: https://doi.org/10.28927/SR.382163.
NI, P.; SONG, L.; MEI, G.; ZHAO, Y. Generalized nonlinear softening load-transfer model for axially loaded piles. ***International Journal of Geomechanics,*** v. 17, n. 8, p. 1-10, 2017. https://doi.org/10.1061/(ASCE)GM.1943-5622.0000899.
ONG, Y. H.; TOH, C. T.; CHEE, S. K.; MOHAMAD, H. (). Bored piles in tropical soils and rocks: shaft and base resistances, t–z and q–w models. ***Proceedings of the Institution of Civil Engineers - Geotechnical Engineering,*** v. 174, n. 2, 193-224, 2021. DOI: https://doi.org/10.1680/jgeen.19.00106.
PETEK, K.; MITCHELL, R.; ELLIS, H. ***FHWA deep foundation load test database version 2.0 user manual.*** Federal Highway Administration, Seattle. 2016. Available at: https://rosap.ntl.bts.gov/view/dot/35880. v. 1.
PHAM, T. A.; LY, H. B.; TRAN, V. Q.; GIAP, L. Van; VU, H.-L. T.; Duong, H. A. T. Prediction of pile axial bearing capacity using artificial neural network and random forest. ***Applied Sciences,*** v. 10, n. 5, p. 1871, 2020. DOI: https://doi.org/10.3390/app10051871.
POULOS, H. G.; DAVIS, E. H. The settlement behaviour of single axially-loaded incompressible piles and piers.

Géotechnique, v. 18, n. 3, p. 351-371. 1968. DOI: https://doi.org/10.1680/geot.1968.18.3.351

REBOLLEDO, J. F. R.; LEÓN, R. F. P.; CAMAPUM, J. Obtaining the mechanical parameters for the hardening soil model of tropical soils in the city of Brasília. ***Soils and Rocks,*** v. 42, n. 1, p. 61-74, 2019. DOI: https://doi.org/10.28927/SR.421061.

ROMÃO, P. de A. Modelagem de terreno com base na morfometria e em sondagens geotécnicas - região de Goiânia - GO. Tese (Doutorado) - Departamento de Engenharia Civil e Ambiental - Universidade de Brasília, Brasília-DF, 2006, 166 f.

SATYANARAYANA, R.; EALY, C. D.; DIMILLIO, A. F.; KALAVAR, S. R. User query interface for the Deep-Foundations Load-Test database. Transportation Research Record: ***Journal of the Transportation Research Board,*** v. 1755, n. 1, 3-14. 2001. DOI: https://doi.org/10.3141/1755-01.

TOMLINSON, M.; WOODWARD, J. ***Pile design and construction practice.*** 5 ed. New York: Taylor & Francis, 2008. 547 p.

UZIELLI, M. Statistical analysis of geotechnical data. *In*: ***Geotechnical and geophysical site characterization.*** CRC Press, 2008. p. 181-202.

VESIC, A. S. Analysis of ultimate loads of shallow foundations. ***Journal of the Soil Mechanics and Foundations Division,*** 99, p. 45-73, 1973. DOI: https://doi.org/10.1061/JSFEAQ.0001846.

ZHANG, J.; HU, J.; LI, X.; LI, J. Bayesian network based machine learning for design of pile foundations. ***Automation in Construction,*** 118, 103295. 2020. DOI: https://doi.org/10.1016/j.autcon.2020.103295.

ZHENG, G.; PENG, S. Y.; NG, C. W. W.; DIAO,Y. Excavation effects on pile behaviour and capacity. ***Canadian Geotechnical Journal,*** v. 49, n. 12, p. 1347-1356. DOI: 2012.https://doi.org/10.1139/t2012-095.

Received: 23 November 2023 - Accepted: 23 October 2024.

Appendix

The Equations (1), (2), and (3) compute the maximum unitary pile skin friction (in kPa) according to the methods of Décourt & Quaresma (1978) , Antunes & Cabral (1996), and Aoki & Velloso (1975), respectively. All the methods are based on the average N_{SPT} values measured around the pile shaft and some empirical coefficients, according to the following equations:

$$q_{l\,max} = 10\left(\frac{N_{SPT}}{3} + 1\right) \tag{1}$$

$$q_{l\,max} = \beta_1 N_{SPT} \tag{2}$$

where β_1 is an empirical coefficient that depends on the soil classification, which is equal to 3.0, 2.5, and 3.5 for the sandy clay, clayey silt, and sandy silt soil types, respectively.

$$q_{l\,max} = 10\left(\frac{\alpha\, k}{F_2}\right) N_{SPT} \tag{3}$$

where α and k are empirical coefficients that depend on the soil type. This study used α values equal to 2.4, 3.4, and 2.2, and k values equal to 0.35, 0.23, and 0.55, for the sandy clay, clayey silt, and sandy silt soil types, respectively (according to Cintra & Aoki, 2010). F2 is a factor to consider the pile installation procedure, which is equal to 4 for CFA piles.

CC BY All content of the journal, except where identified, is licensed under a Creative Commons attribution-type BY.